Electronic Supplementary Material (ESI) for Dalton Transactions.

Supporting Information

Facile mechanochemical synthesis of MIL-53 and its isoreticular analogues with a glance at reaction reversibility

Fillipp Edvard Salvador,[a,◊] Zhuorigebatu Tegudeer,[b,◊] Halie Locke [a] and Wen-Yang Gao*[b]

[a] *Department of Chemistry, New Mexico Institute of Mining and Technology, Socorro, New Mexico 87801, United States*

[b] *Department of Chemistry and Biochemistry, Ohio University, Athens, Ohio 45701, United States*

◊ *These two authors contributed equally.*

Email: gaow@ohio.edu

Table of Contents

A. General Considerations

Materials Solvents were obtained as ACS reagent grade and used as received. Unless otherwise noted, all chemicals and solvents were used as received. *N,N*-Dimethyl formamide (DMF) was obtained from J.T. Baker. Methanol (MeOH) was obtained from VWR Chemicals BDH. Benzene-1,4-dicarboxylic acid and aluminum(III) nitrate ($Al(NO_3)_3$) were obtained from Acros Organics. Indium(III) sulfate hydrate was obtained from Alfa Aesar. Aluminum(III) sulfate octadecahydrate ($Al_2(SO_4)_3{\cdot}18H_2O$), aluminum(III) hydroxide ($Al(OH)_3$), 2-aminobenzene-1,4-dicarboxylic acid, and 2,5-bis(trifluoromethyl)benzene-1,4-dicarboxylic acid were obtained from AmBeed. Diacetoxy(hydroxy)aluminum ($Al(OH)(OAc)_2$), gallium(III) sulfate hydrate, and fumaric acid were obtained from Beantown Chemical. 2-Methylfumaric acid was obtained from Combi-Blocks. Sodium hydroxide (NaOH) was obtained from Oakwood Chemical. UHP-grade N_2 and He, used in gas adsorption measurements, were obtained from Airgas. All reactions were carried out under an ambient atmosphere unless otherwise noted.

Mechanochemical Synthesis Mechanochemical synthesis was conducted using a Retsch Mixer Mill MM 400. Starting materials were loaded into a 10 mL Teflon grinding jar with 2 Teflon grinding balls (10 mm Ø) and milled at a frequency of 30 Hz.

Characterization Details Infrared (IR) spectra were recorded on a Thermo Nicolet Avatar 370 DTGS spectrometer with a SMART PERFORMER ATR module. Spectra were blanked against air and were determined as the average of 64 scans. Powder X-ray Diffraction (PXRD) measurements were carried out on a Panalytical X'Pert Pro Diffractometer (Cu Kα, 1.5406 Å; 45 kV, 40 mA; the angular range was measured from 4.00 to 50.00° (2θ) with steps of 0.017° and a measurement time of 0.4 second per step) or Rigaku Miniflex II (Cu Kα, 1.5406 Å; 30 kV, 15 mA; the angular range was measured from 4.00 to 50.00° (2θ) with a sampling width of 0.1° and a scan speed of 3.00° per minute). Simulated PXRD patterns were calculated using Mercury 3.9.[1] The average crystallite size D of the sample is calculated from the Scherrer equation: $D = K\lambda/(\beta\cos\theta)$, where K is the Debye-Scherrer constant ($K = 0.9$), λ is the X-ray wavelength ($\lambda = 0.15406$ nm), β is the peak width of half-maximum, and θ is the Bragg diffraction angle. Thermogravimetric analysis (TGA) was performed on a Shimadzu DTG-60 analyzer with a ramping rate of 15 °C/min.

Gas Adsorption Details N_2 adsorption isotherms (0−1.0 bar pressure range) were measured volumetrically at 77 K using a Quantachrome Autosorb-iQ. The synthesized samples underwent solvent exchange with MeOH for 3 d (10 mL × 9). The solvent-exchanged samples were transferred under N_2 atmosphere to pre-weighed analysis tubes. The sample was evacuated at 150 °C until the outgas rate was <10 μbar/min and further maintained for 16 h. The tube was weighed to determine the mass of the activated sample. The tube was transferred to the analysis port of the instrument. UHP-grade (99.999% purity) N_2 and He were used for all adsorption measurements. Brunauer-Emmett-Teller (BET) surface areas were calculated in relative pressure range 0.007 to 0.03. The pore size distribution plots are reported by both dV(d) and cumulative pore volume calculated by N_2 adsorption isotherms using the non-local density functional theory (NLDFT) cylindrical pore silica model.

B. Synthesis and Characterization

Mechanochemical Synthesis of [Al(OH)(bdc)]

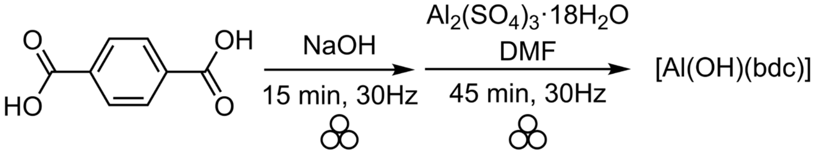

A 10-mL Teflon grinding jar was charged with 2 Teflon grinding balls, benzene-1,4-dicarboxylic acid (H_2bdc, 0.050 g, 0.30 mmol, 2.0 equiv), and NaOH (0.036 g, 0.90 mol, 6.0 equiv). The resulting mixture was milled for Retsch Mixer Mill MM 400 at 30 Hz for 15 min then $Al_2(SO_4)_3\cdot18H_2O$ (0.100 g, 0.150 mmol, 1.00 equiv) and *N,N*-dimethylformamide (DMF, 56 µL, η = 0.30 µL/mg) were added to the grinding jar. The mixture was further milled for 45 min. The obtained solids were collected and washed by water (10 mL × 3) and MeOH (10 mL × 3). The solids were dried under reduced pressure to afford [Al(OH)(bdc)] (0.056 g, 90% yield) as a white powder. Primary data are presented below: PXRD, Figures 2 and S1–S4; IR, Figure S5; N_2 adsorption isotherm, Figure 2b; TGA, Figure S6; pore size distribution, Figure S37.

Mechanochemical Synthesis of [Al(OH)(fum)]

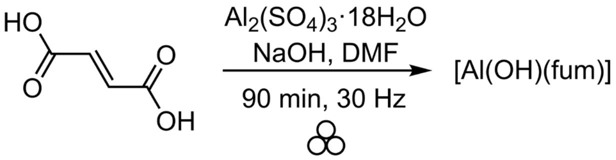

A 10-mL Teflon grinding jar was charged with 2 Teflon grinding balls, $Al_2(SO_4)_3\cdot 18H_2O$ (0.086 g, 0.13 mmol, 1.0 equiv), fumaric acid (H_2fum, 0.030 g, 0.26 mmol, 2.0 equiv), NaOH (0.031 g, 0.78 mmol, 6.0 equiv), and DMF (89 µL, η = 0.60 µL/mg). The resulting mixture was milled using a Retsch Mixer Mill MM 400 at 30 Hz for 90 min. The obtained solids were collected and washed by water (10 mL × 3) and MeOH (10 mL × 3). The solids were dried under reduced pressure to afford [Al(OH)(fum)] (0.032 g, 78% yield) as a white powder. Primary data are presented below: PXRD, Figures 3 and S7–S9; IR, Figure S10; TGA, Figure S11; N_2 adsorption isotherm, Figure S12.

Mechanochemical Synthesis of [Al(OH)(NH_2bdc)]

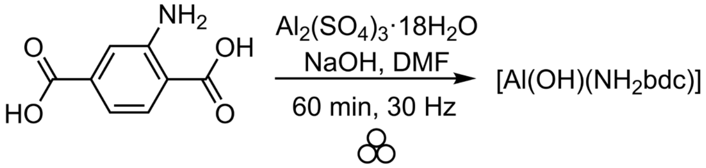

A 10-mL Teflon grinding jar was charged with 2 Teflon grinding balls, $Al_2(SO_4)_3 \cdot 18H_2O$ (0.077 g, 0.12 mmol, 1.0 equiv), 2-aminobenzene-1,4-dicarboxylic acid (H_2NH_2bdc, 0.042 g, 0.24 mmol, 2.0 equiv), NaOH (0.029 g, 0.72 mol, 6.0 equiv), and DMF (22 μL, η = 0.15 μL/mg). The resulting mixture was milled using a Retsch Mixer Mill MM 400 at 30 Hz for 60 min. The obtained solids were collected and washed by water (10 mL × 3) and MeOH (10 mL × 3). The solids were dried under reduced pressure to afford [Al(OH)(NH_2bdc)] (0.043 g, 83% yield) as a pale yellow powder. Primary data are presented below: PXRD, Figures 3, S13-15; IR, Figure S16; N_2 adsorption isotherm, Figure S17; TGA, Figure S18.

Mechanochemical Synthesis of [Al(OH)(btfmbdc)]

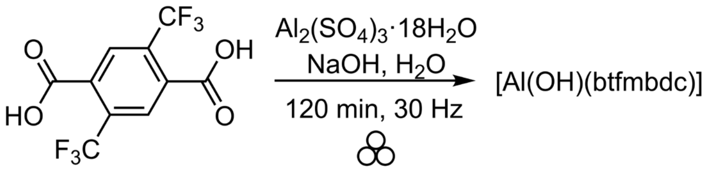

A 10-mL Teflon grinding jar was charged with 2 Teflon grinding balls, 2,5-bis(trifluoromethyl)benzene-1,4-dicarboxylic acid (H_2btfmbdc, 0.040 g, 0.13 mmol, 2.0 equiv), NaOH (0.016 g, 0.397 mmol, 6.0 equiv), $Al_2(SO_4)_3 \cdot 18H_2O$ (0.044 g, 0.066 mmol, 1.0 equiv) and H_2O (15 μL, η = 0.15 μL/mg). The resulting mixture was milled using a Retsch Mixer Mill MM 400 at 30 Hz for 120 min. The obtained product was collected and washed with water (10 mL × 3), and then MeOH (10 mL × 3). The solids were dried under reduced pressure to afford [Al(OH)(btfmbdc)] (0.032 g, 72% yield) as a white powder. Primary data are presented below: PXRD, Figures 3, S19-21; IR, Figure S22; TGA, Figure S23.

Mechanochemical Synthesis of [Al(OH)(mfum)]

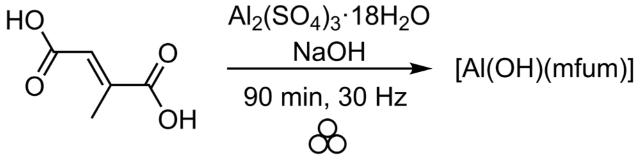

A 10-mL Teflon grinding jar was charged with 2 Teflon grinding balls, $Al_2(SO_4)_3 \cdot 18H_2O$ (0.095 g, 0.14 mmol, 1.0 equiv), 2-methylfumaric acid (H_2mfum, 0.037 g, 0.28 mmol, 2.0 equiv), NaOH (0.034 g, 0.84 mmol, 6.0 equiv). The resulting mixture was milled using a Retsch Mixer Mill MM 400 at 30 Hz for 90 min. The obtained product was collected and washed by water (10 mL × 3) and MeOH (10 mL × 3). The solids were dried under reduced pressure to afford [Al(OH)(mfum)] (0.020 g, 41% yield) as a white powder. Primary data are presented below: PXRD, Figures 3, S24-25; IR, Figure S26; N_2 adsorption isotherm, Figure S27; TGA, Figure S28.

Mechanochemical Synthesis of [In(OH)(fum)]

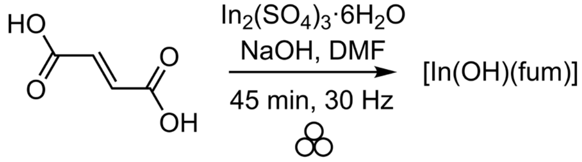

A 10-mL Teflon grinding jar was charged with 2 Teflon grinding balls, $In_2(SO_4)_3·6H_2O$[a] (0.067 g, 0.13 mmol, 1.0 equiv), H_2fum (0.030 g, 0.26 mmol, 2.0 equiv), NaOH (0.031 g, 0.78 mmol, 6.0 equiv), and DMF (77 µL, η = 0.60 µL/mg). The resulting mixture was milled using a Retsch Mixer Mill MM 400 at 30 Hz for 45 min. The obtained product was collected and washed by H_2O (5 mL × 1) and MeOH (10 mL × 3). The solids were dried under reduced pressure to afford [In(OH)(fum)] (0.029 g, 46% yield) as a white powder. Primary data are presented below: PXRD, Figures 4a and S29; IR, Figure S30.

---

[a] The hydrate formula was calculated based on the thermogravimetric analysis plot of commercial indium(III) sulfate hydrate.

Mechanochemical Synthesis of [Ga(OH)(fum)]

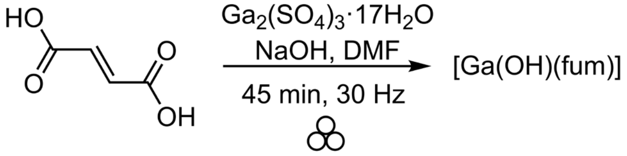

A 10-mL Teflon grinding jar was charged with 2 Teflon grinding balls, $Ga_2(SO_4)_3 \cdot 17H_2O$[b] (0.063 g, 0.086 mmol, 1.0 equiv), fumaric acid (H_2fum, 0.020 g, 0.17 mmol, 2.0 equiv), NaOH (0.021 g, 0.52 mmol, 6.0 equiv), and DMF (43 μL, η = 0.40 μL/mg). The resulting mixture was milled using a Retsch Mixer Mill MM 400 at 30 Hz for 45 min. The obtained product was collected and washed by H_2O (5 mL × 1) and MeOH (10 mL × 3). The solids were dried under reduced pressure to afford [Ga(OH)(fum)] (0.020 g, 59% yield) as a white powder. Primary data are presented below: PXRD, Figures 3, S32-33; IR, Figure S30; N_2 adsorption isotherm, Figure S36.

---

[b] The hydrate formula was calculated based on the thermogravimetric analysis plot of commercial gallium(III) sulfate hydrate.

C. Supporting Figures

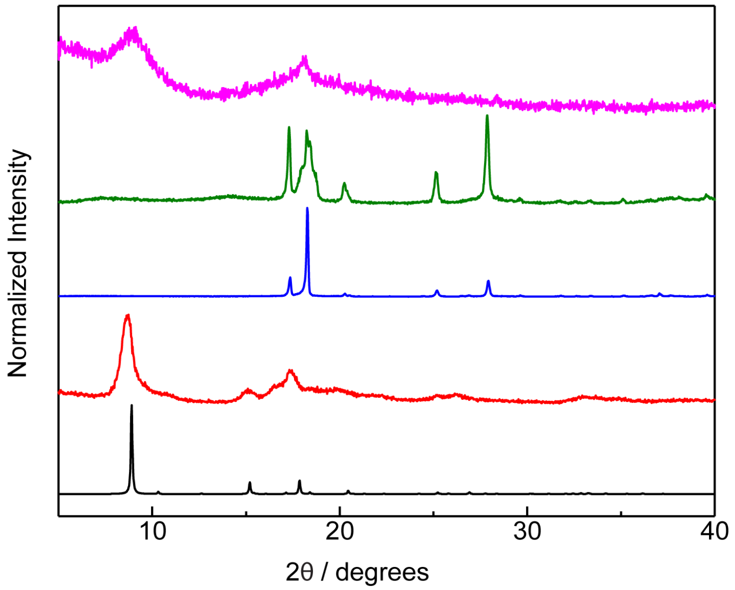

Figure S1. PXRD patterns were collected on the mechanochemically obtained solids by the employment of various aluminum precursors, including $Al_2(SO_4)\cdot 18H_2O$ (—), $Al(OH)_3$ (—), $Al(OH)(OAc)_2$ (—), or $Al(NO_3)_3$ (—) along with stoichiometric amounts of H_2bdc and NaOH, as well as DMF (η = 0.30 μL/mg) at 30 Hz for 60 min. Compared against the calculated patterns of [Al(OH)(bdc)] (—), only the reaction using $Al_2(SO_4)\cdot 18H_2O$ produces the desired MIL-53 phase.

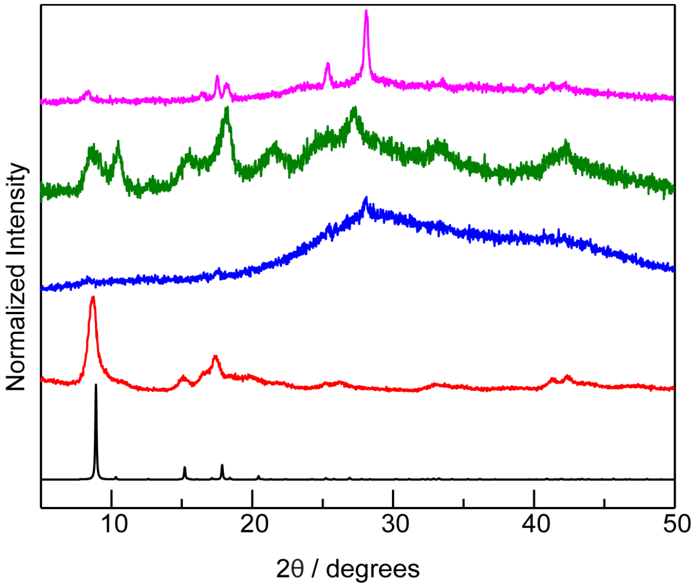

Figure S2. PXRD patterns were collected on the mechanochemically obtained solids by the employment of various liquid additives (η = 0.30 μL/mg) including DMF (—), H_2O (—), MeOH (—), or neat (—) along with stoichiometric amounts of $Al_2(SO_4)\cdot18H_2O$, H_2bdc and NaOH at 30 Hz for 60 min. Compared against the calculated patterns of [Al(OH)(bdc)] (—), the choice of DMF as the additive liquid produces the desired MIL-53 phase.

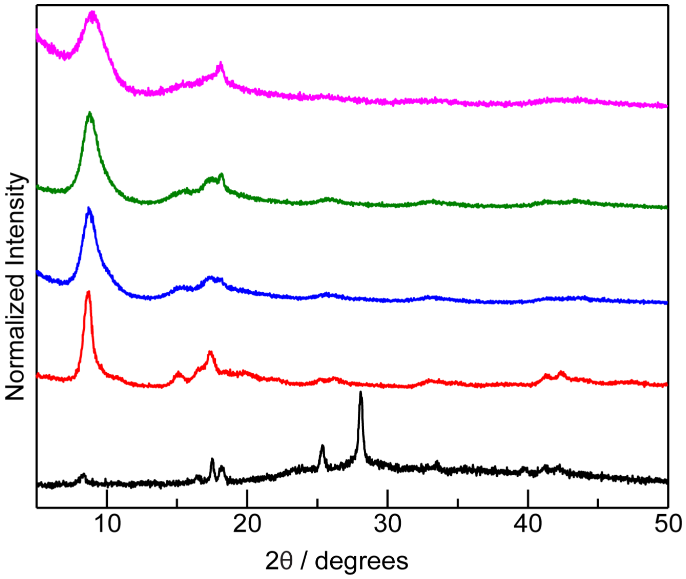

Figure S3. PXRD patterns were collected on the mechanochemically obtained solids by the employment of different amounts of DMF, including η = 0 μL/mg (—) or the neat condition, η = 0.30 μL/mg (—), η = 0.45 μL/mg (—), η = 0.60 μL/mg (—), and η = 0.90 μL/mg along with stoichiometric amounts of $Al_2(SO_4)\cdot 18H_2O$, H_2bdc and NaOH at 30 Hz for 60 min. The most quality PXRD patterns based on peak width were generated by the amount of DMF at 0.30 μL/mg.

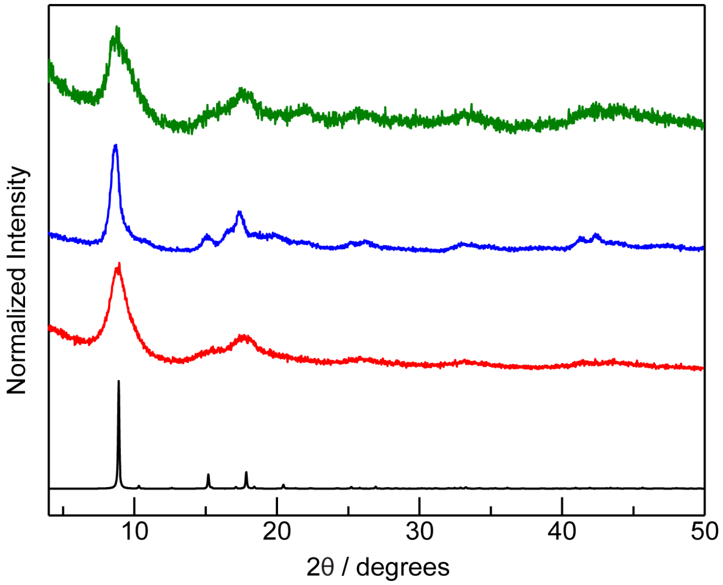

Figure S4. PXRD patterns were collected on the mechanochemically obtained solids by the employment of different milling time, including 30 min (—), 60 min (—), and 90 min (—), along with stoichiometric amounts of $Al_2(SO_4)\cdot 18H_2O$, H_2bdc and NaOH, as well as DMF (η = 0.30 μL/mg) at 30 Hz. The most quality PXRD patterns based on peak width were generated by the milling time of 60 min.

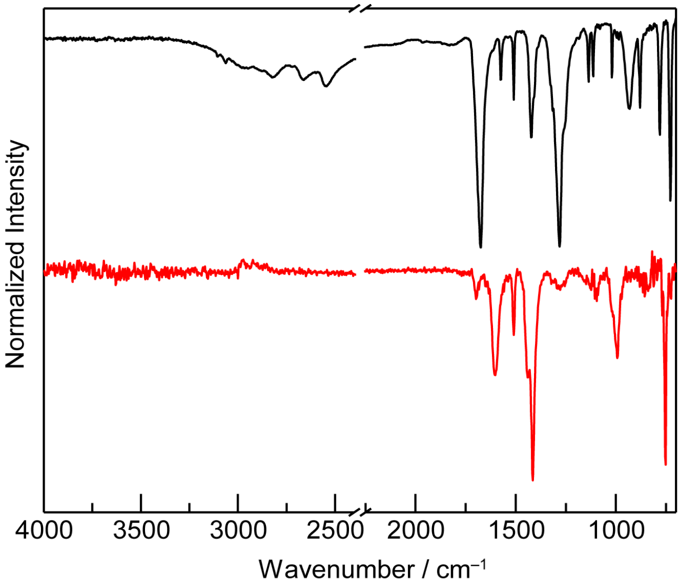

Figure S5. IR spectra (4000–700 cm^{-1} with a break between 2400 and 2250 cm^{-1}) were collected from [Al(OH)(bdc)] (—) and H$_2$bdc (—). The mechanochemically obtained [Al(OH)(bdc)] lacks the broad O–H stretching between 2500 and 3300 cm^{-1} and the uncoordinated carbonyl stretching at 1675 cm^{-1}, indicating the formation of an extended framework.

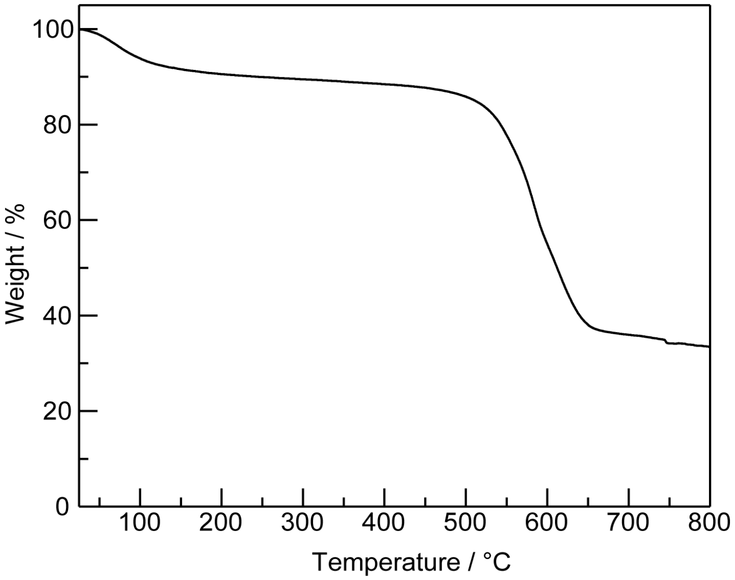

Figure S6. A plot of weight% vs. temperature was recorded by thermogravimetric analysis of the mechanochemically obtained [Al(OH)(bdc)].

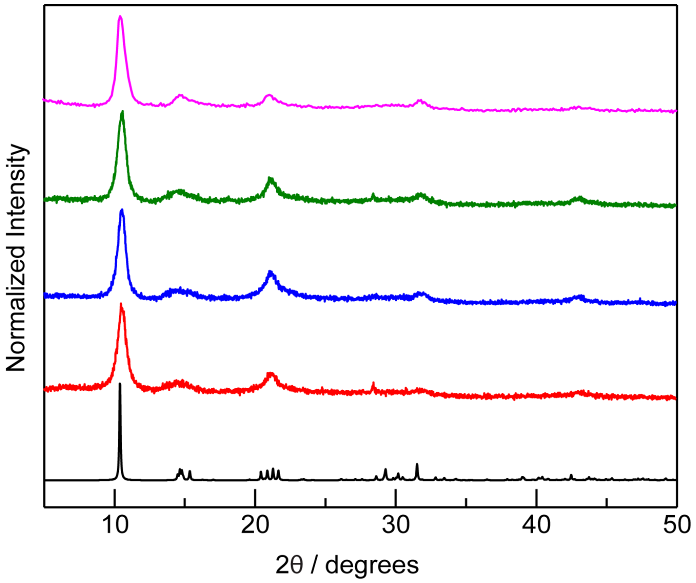

Figure S7. PXRD patterns were collected on the mechanochemically obtained [Al(OH)(fum)] by the employment of different liquid additives (η = 0.30 µL/mg), including DMF (—), H_2O (—), and MeOH (—), or neat (—) along with stoichiometric amounts of $Al_2(SO_4)\cdot 18H_2O$, H_2fum and NaOH at 30 Hz for 60 min. Compared against the calculated patterns for [Al(OH)(fum)] (—), the type of liquid additive does not significantly impact the quality of resultant PXRD patterns.

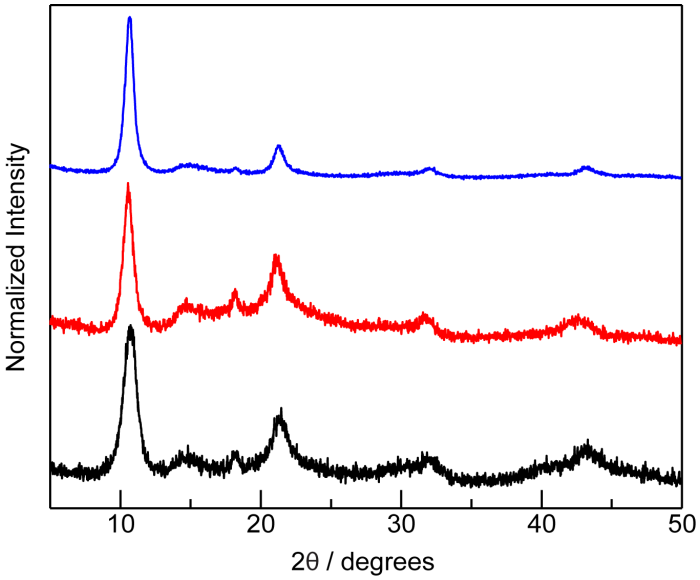

Figure S8. PXRD patterns were collected on [Al(OH)(fum)] samples prepared by different milling time, 30 min (—), 60 min (—), and 90 min (—), with the presence of DMF (η = 0.60 μL/mg) and NaOH (6.0 equiv) and a frequency of 30 Hz. Milling for 90 min gives the material with the best crystallinity.

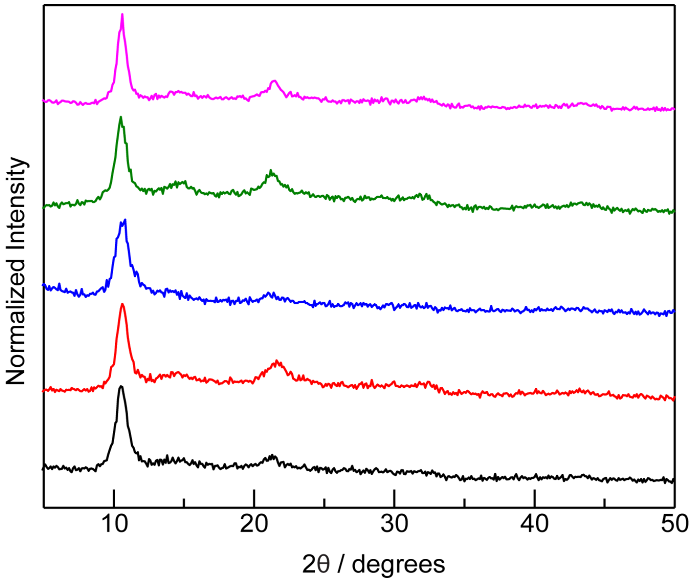

Figure S9. PXRD patterns were collected on [Al(OH)(fum)] samples obtained by adding different amount of DMF, η = 0.30 μL/mg (—) and η = 0.60 μL/mg (—), η = 0.90 μL/mg (—), η = 1.2 μL/mg (—), and η = 1.5 μL/mg (—), with the presence of NaOH (6.0 equiv) and a frequency of 30 Hz for 45 min. The amount of DMF (between η = 0.3 μL/mg and η = 1.5 μL/mg) does not seem to impact the crystallinity significantly.

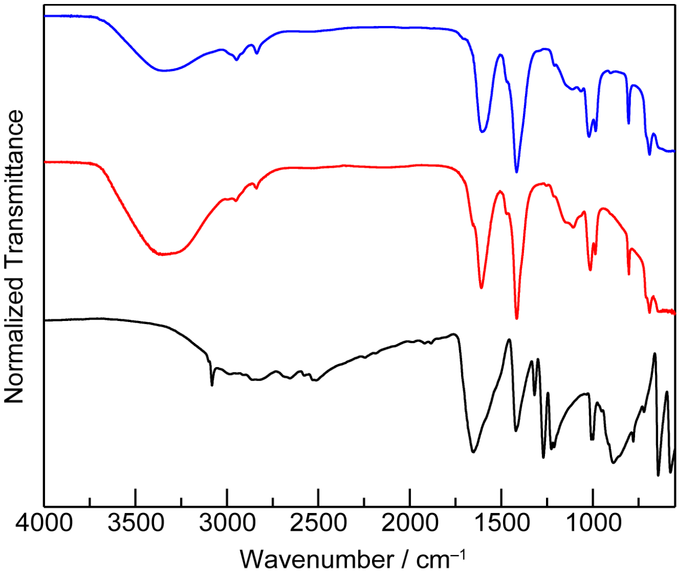

Figure S10. IR spectra of (4000–700 cm^{-1}) were collected from H_2fum (—) and the mechanochemically obtained [Al(OH)(fum)] (— prior to MeOH exchange evidenced by the presence of DMF with carbonyl stretch around 1650 cm^{-1} as a shoulder peak and — after MeOH exchange in the absence of DMF).

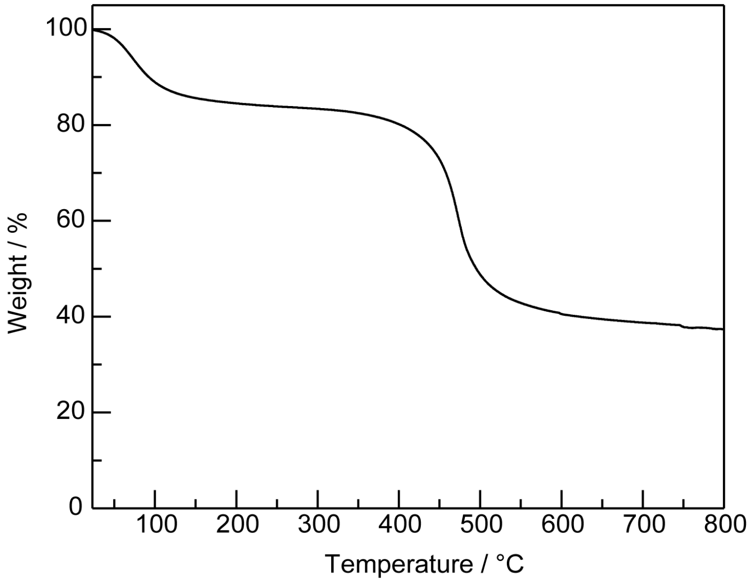

Figure S11. A plot of weight% vs. temperature was obtained by thermogravimetric analysis of the mechanochemically synthesized [Al(OH)(fum)].

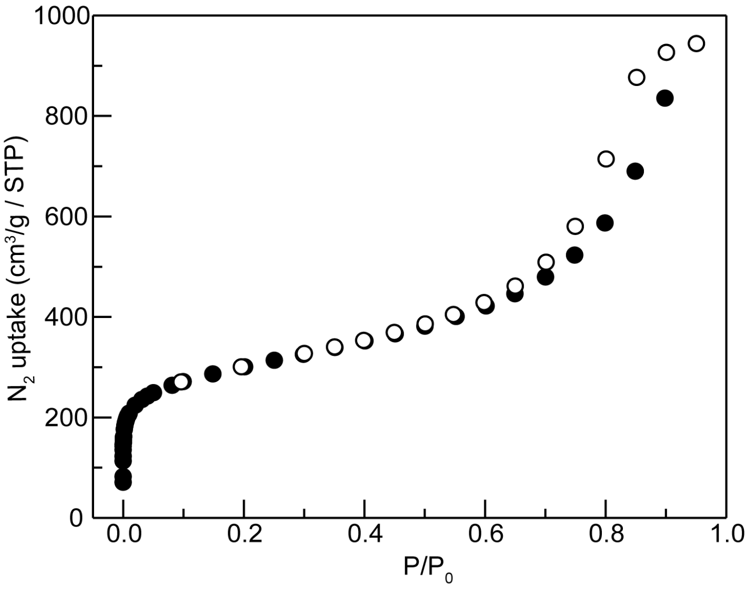

Figure S12. N_2 adsorption isotherm (adsorption (●), desorption (○)) at 77 K was collected from [Al(OH)(fum)]. The Brunauer-Emmett-Teller (BET) surface area was calculated as 1080 m^2/g (P/P$_0$ = 0.007 to 0.03).

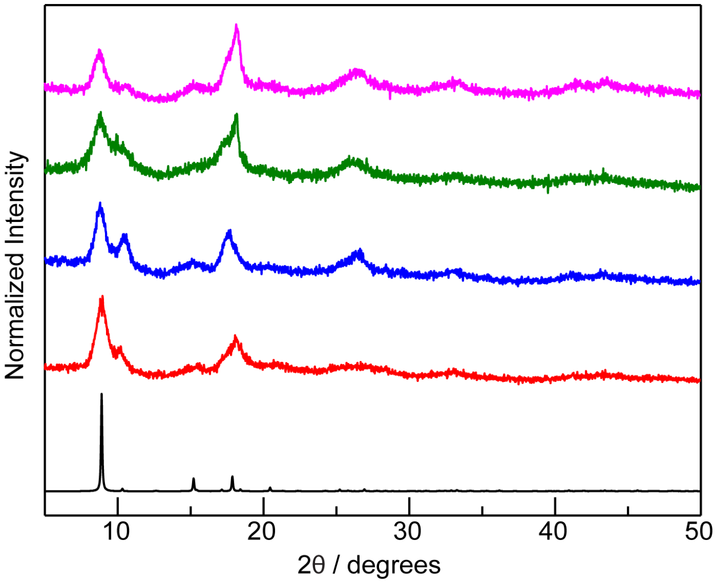

Figure S13. PXRD patterns were collected on the mechanochemically obtained [Al(OH)(NH$_2$bdc)] by the employment of various liquid additives (η = 0.30 μL/mg) including DMF (—), H_2O (—), MeOH (—), or neat (—) along with stoichiometric amounts of $Al_2(SO_4)\cdot18H_2O$, H$_2$NH$_2$bdc and NaOH at 30 Hz for 60 min. Compared against the calculated patterns of [Al(OH)(bdc)] (—), the choice of DMF as the additive liquid produces the desired MIL-53 phase with the best quality PXRD patterns.

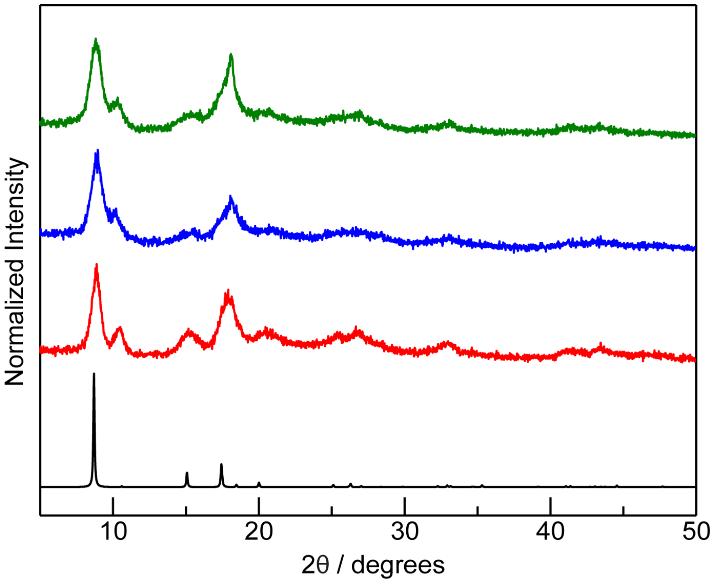

Figure S14. PXRD patterns were collected on the mechanochemically obtained [Al(OH)(NH$_2$bdc)] by the employment of different loadings of DMF, including η = 0.15 μL/mg (—), η = 0.30 μL/mg (—), and η = 0.60 μL/mg (—) along with stoichiometric amounts of Al$_2$(SO$_4$)·18H$_2$O, H$_2$NH$_2$bdc and NaOH at 30 Hz for 60 min. Compared against the calculated patterns of isostructural [Al(OH)(bdc)] (—), the most quality PXRD patterns based on peak width were generated by the amount of DMF at 0.15 μL/mg.

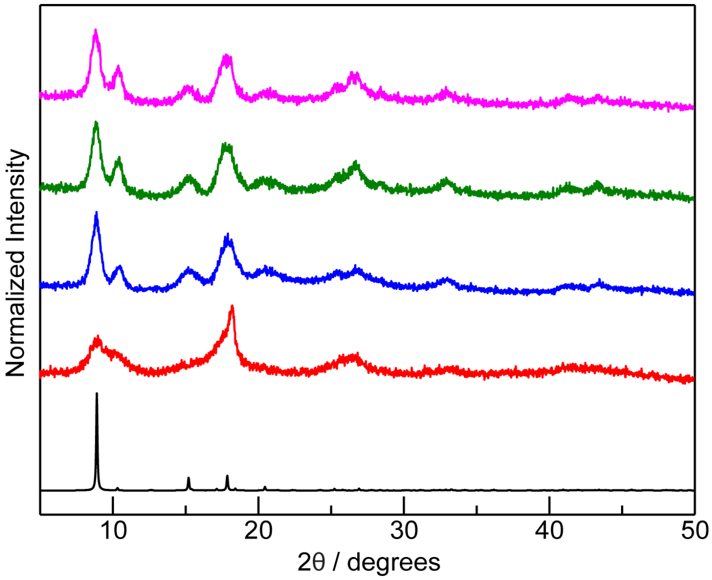

Figure S15. PXRD patterns were collected on the mechanochemically obtained [Al(OH)(NH_2bdc)] by the employment of different milling time, including 30 min (—), 60 min (—), 90 min (—), and 120 min (—) , along with stoichiometric amounts of $Al_2(SO_4)·18H_2O$, H_2NH_2bdc and NaOH, as well as DMF (η = 0.15 μL/mg) at 30 Hz. Compared against the calculated patterns of isostructural [Al(OH)(bdc)] (—), this mechanochemical reaction requires at least 60 min to afford the quality PXRD patterns based on peak width.

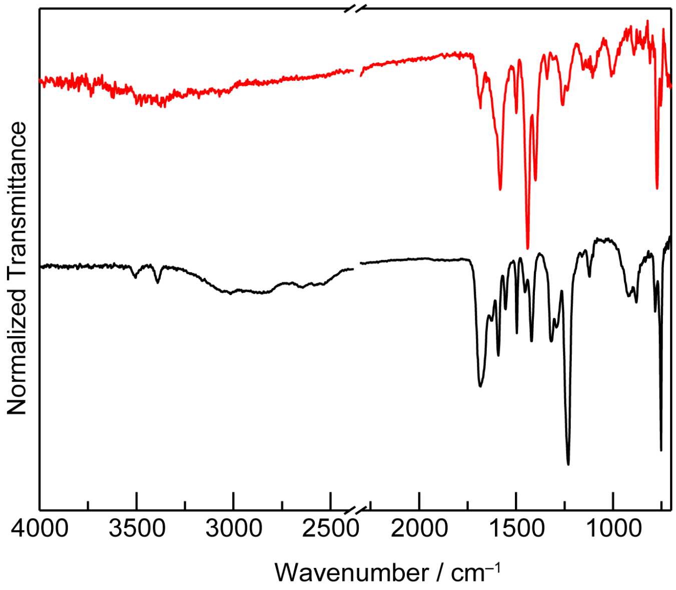

Figure S16. IR spectra (4000–700 cm^{-1} with a break between 2400 and 2300 cm^{-1}) were collected from $[\mathrm{Al(OH)(NH_2bdc)}]$ (—) and $\mathrm{H_2NH_2bdc}$ (—). The mechanochemically obtained $[\mathrm{Al(OH)(NH_2bdc)}]$ lacks the broad O–H stretching between 2500 and 3300 cm^{-1} and the uncoordinated carbonyl stretching at 1682 cm^{-1}, indicating the formation of an extended framework.

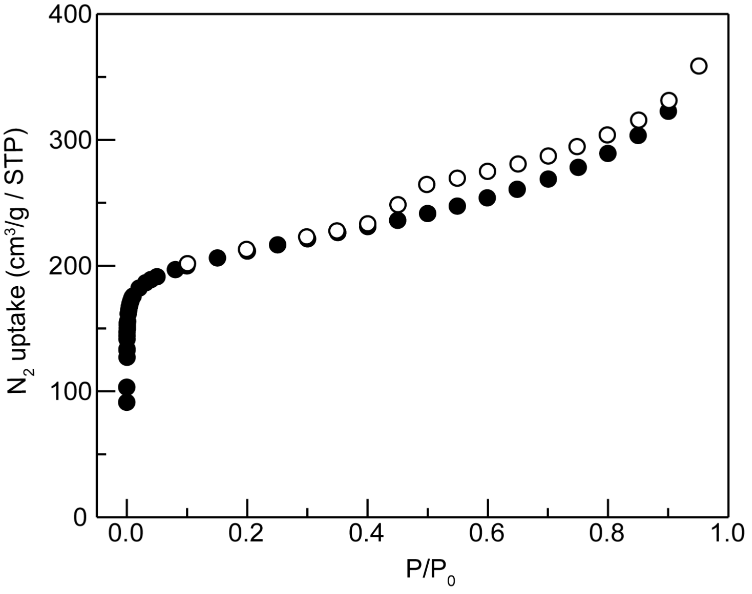

Figure S17. N_2 adsorption isotherm (adsorption (●), desorption (○)) at 77 K was collected from [Al(OH)(NH_2bdc)]. The Brunauer-Emmett-Teller (BET) surface area was calculated as 860 m^2/g (P/P_0 = 0.007 to 0.03).

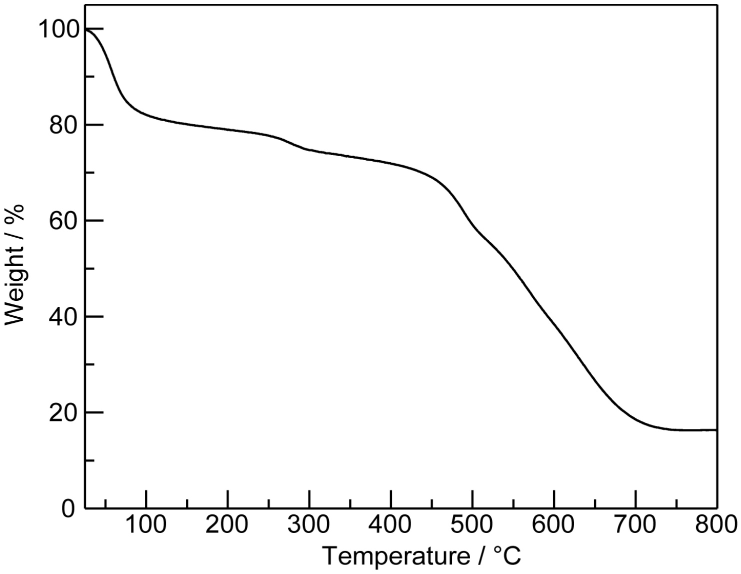

Figure S18. A plot of weight% vs. temperature was recorded by thermogravimetric analysis of the mechanochemically obtained [Al(OH)(NH_2bdc)].

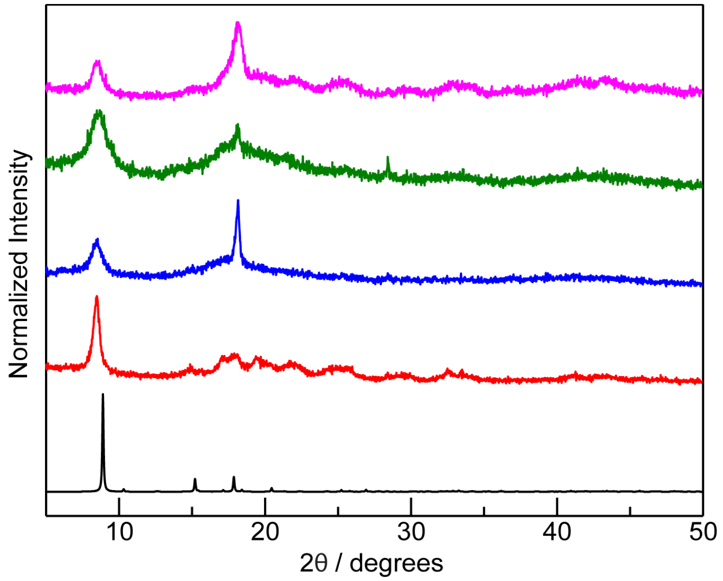

Figure S19. PXRD patterns were collected on the mechanochemically obtained solids by the employment of various liquid additives (η = 0.30 μL/mg) including H_2O (—), DMF (—), MeOH (—), or neat (—) along with stoichiometric amounts of $Al_2(SO_4)\cdot 18H_2O$, H_2btfmbdc and NaOH at 30 Hz for 60 min. Compared against the calculated patterns of [Al(OH)(bdc)] (—), the choice of H_2O as the additive liquid produces the desired [Al(OH)(btfmbdc)] phase isostructural to MIL-53.

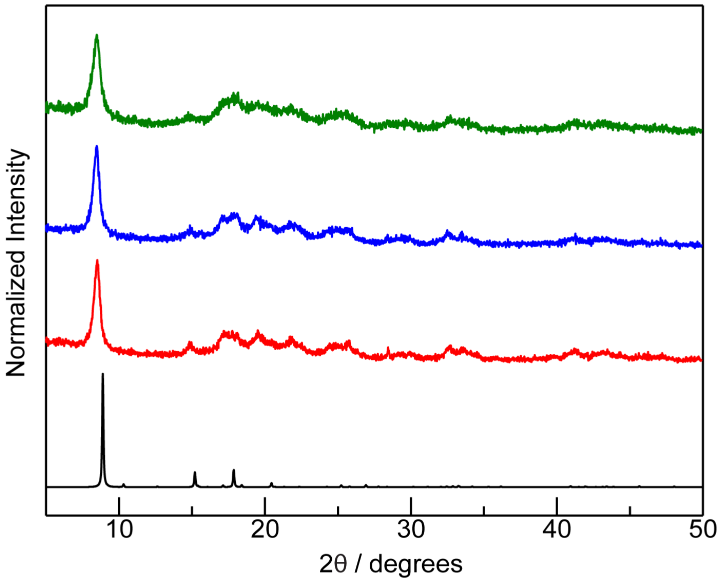

Figure S20. PXRD patterns were collected on the mechanochemically obtained [Al(OH)(btfmbdc)] by the employment of different amounts of H_2O, including $\eta = 0.15$ μL/mg (—), $\eta = 0.30$ μL/mg (—), and $\eta = 0.60$ μL/mg (—) along with stoichiometric amounts of $Al_2(SO_4)\cdot 18H_2O$, H_2btfmbdc and NaOH at 30 Hz for 60 min. These patterns are compared against the calculated pattern of the isostructural [Al(OH)(bdc)] (—) . While the amount of H_2O does not greatly affect the crystallinity of the resulting material, $\eta = 0.15 – 0.30$ μL/mg seems to be sufficient to promote the generation of quality crystalline phase.

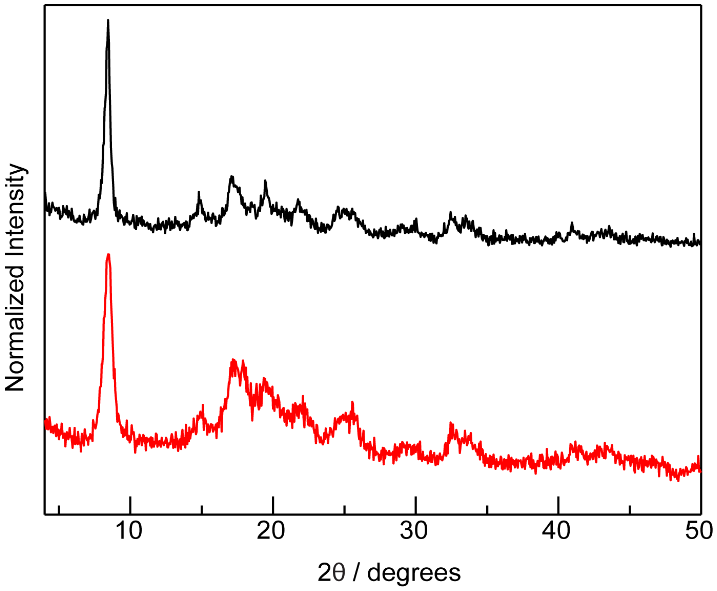

Figure S21. The milling time of 90 min (—) to 120 min (—) were also examined along with stoichiometric amounts of $Al_2(SO_4)\cdot 18H_2O$, H_2btfmbdc and NaOH, as well as H_2O (η = 0.15 μL/mg) at 30 Hz. The better quality PXRD patterns based on peak width were generated by the milling time of 120 min.

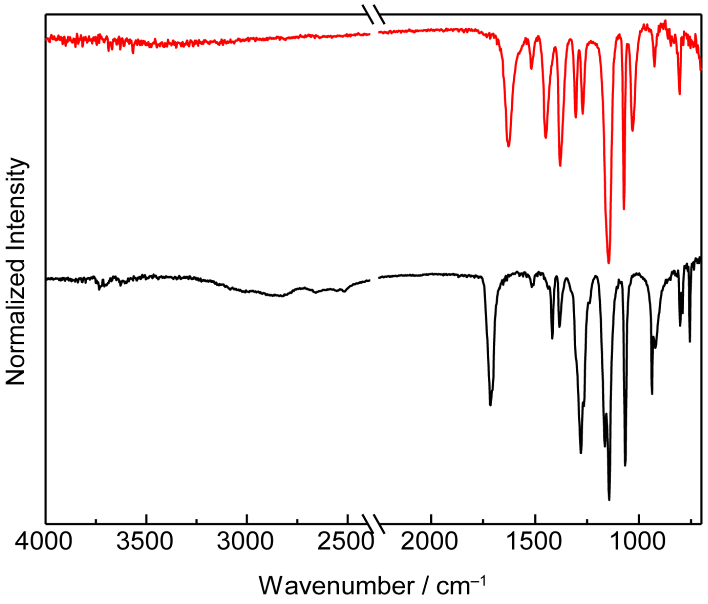

Figure S22. IR spectra (4000–700 cm^{-1} with a break between 2400 and 2200 cm^{-1}) were collected from [Al(OH)(btfmbdc)] (—) and H$_2$btfmbdc (—). The mechanochemically obtained [Al(OH)(btfmbdc)] lacks the broad O–H stretching between 2500 and 3300 cm^{-1} and the uncoordinated carbonyl stretching at 1714 cm^{-1}, indicating the formation of an extended framework.

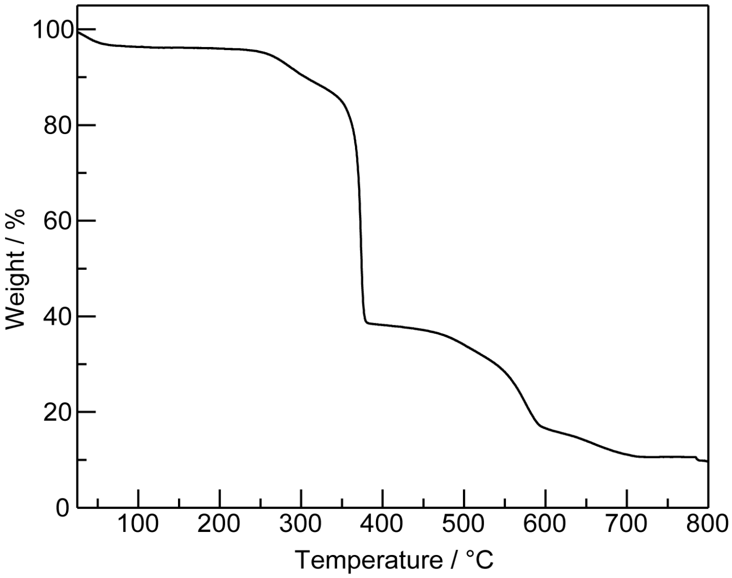

Figure S23. A plot of weight% vs. temperature was recorded by thermogravimetric analysis of the mechanochemically obtained [Al(OH)(btfmbdc)].

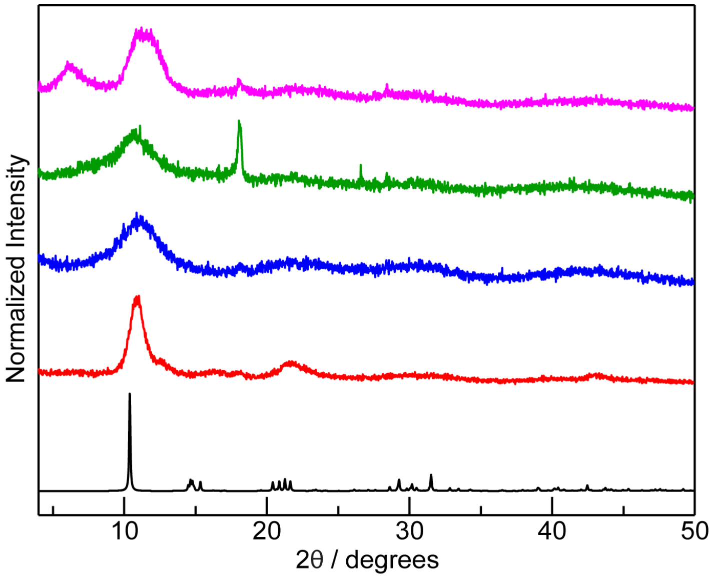

Figure S24. PXRD patterns were collected on the mechanochemically obtained solids by the employment of various liquid additives (η = 0.30 µL/mg) including H_2O (—), DMF (—), MeOH (—), or neat (—) along with stoichiometric amounts of $Al_2(SO_4)\cdot 18H_2O$, H_2mfum and NaOH at 30 Hz for 60 min. Compared against the calculated patterns of the isostructural [Al(OH)(fum)] (—), the choice of the neat condition as the additive liquid produces the desired [Al(OH)(mfum)].

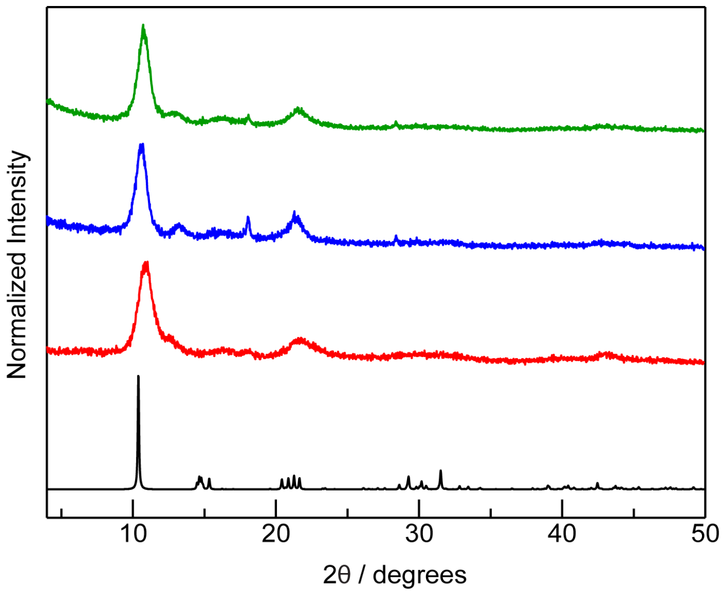

Figure S25. The effect of different milling times, including 60 min (—), 90 min (—), and 120 min (—), on the crystallinity of mechanochemically prepared [Al(OH)(mfum)] was evaluated by PXRD. These patterns are compared against the calculated patterns of the isostructural [Al(OH)(fum)] (—).

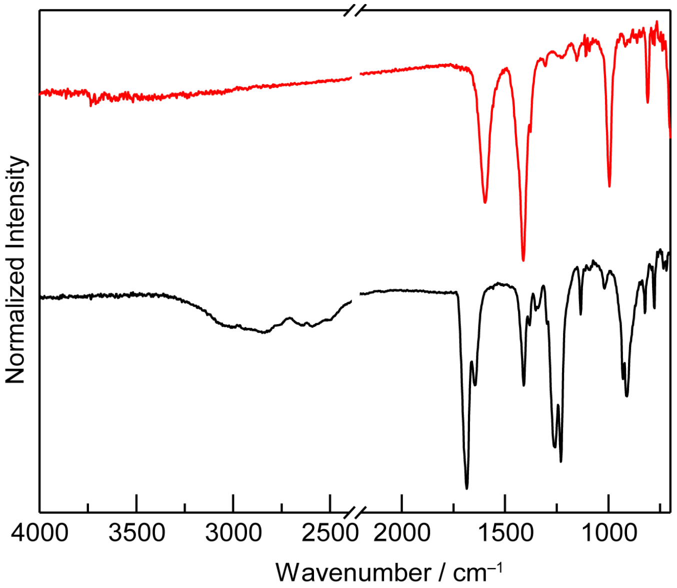

Figure S26. IR spectra (4000–700 cm^{-1} with a break between 2400 and 2200 cm^{-1}) were collected from [Al(OH)(mfum)] (—) and H_2mfum (—). The mechanochemically obtained [Al(OH)(mfum)] lacks the broad O–H stretching between 2500 and 3300 cm^{-1} and the uncoordinated carbonyl stretching at 1684 cm^{-1}, indicating the formation of an extended framework.

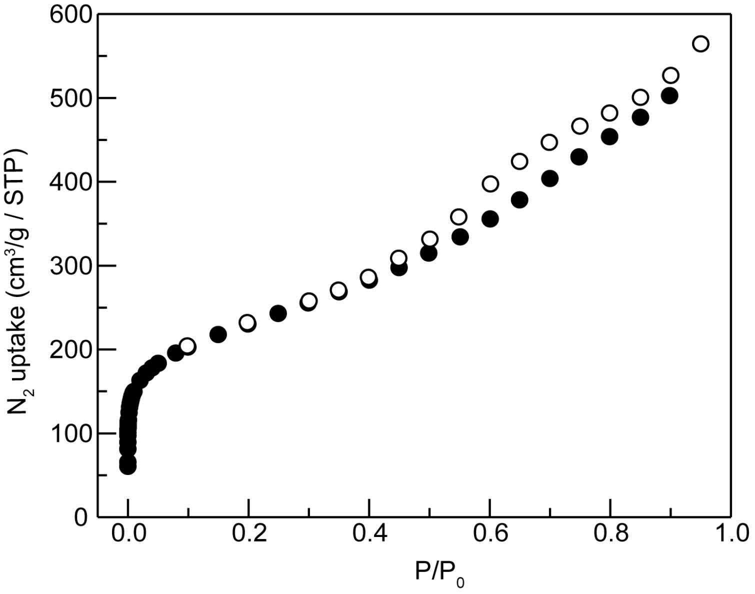

Figure S27. N_2 adsorption isotherm (adsorption (●), desorption (○)) at 77 K was collected from [Al(OH)(mfum)]. The Brunauer-Emmett-Teller (BET) surface area was calculated as 770 m^2/g (P/P$_0$ = 0.007 to 0.03).

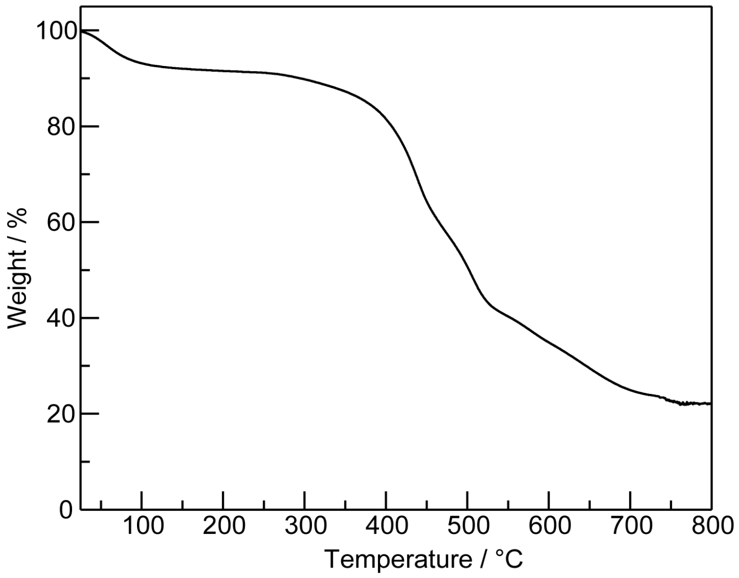

Figure S28. A plot of weight% vs. temperature was recorded by thermogravimetric analysis of the mechanochemically obtained [Al(OH)(mfum)].

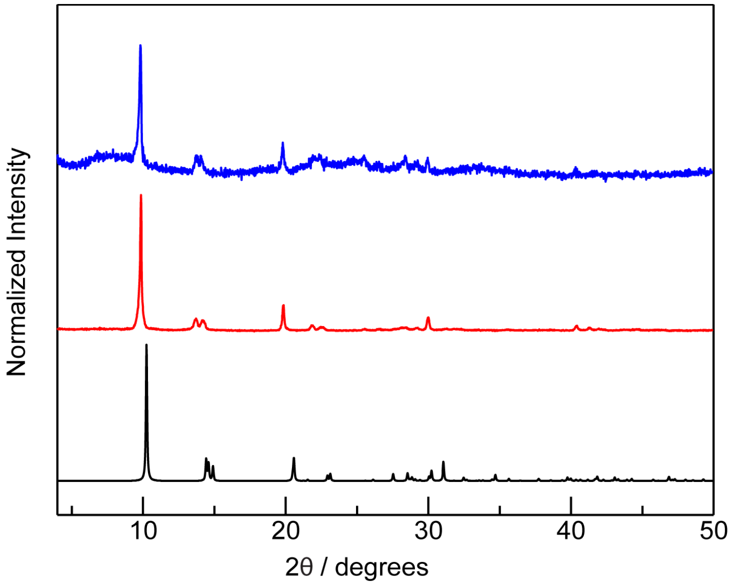

Figure S29. PXRD patterns were collected on the mechanochemically obtained [In(OH)(fum)] by the employment of different amounts of DMF, including η = 0.30 μL/mg (—) and η = 0.60 μL/mg (—), along with stoichiometric amounts of $In_2(SO_4)\cdot6H_2O$, H_2fum and NaOH at 30 Hz for 45 min. Compared against the calculated patterns of the isostructural Ga(OH)(fum) (—), the more quality PXRD patterns of [In(OH)(fum)] were generated by the amount of DMF at 0.60 μL/mg.

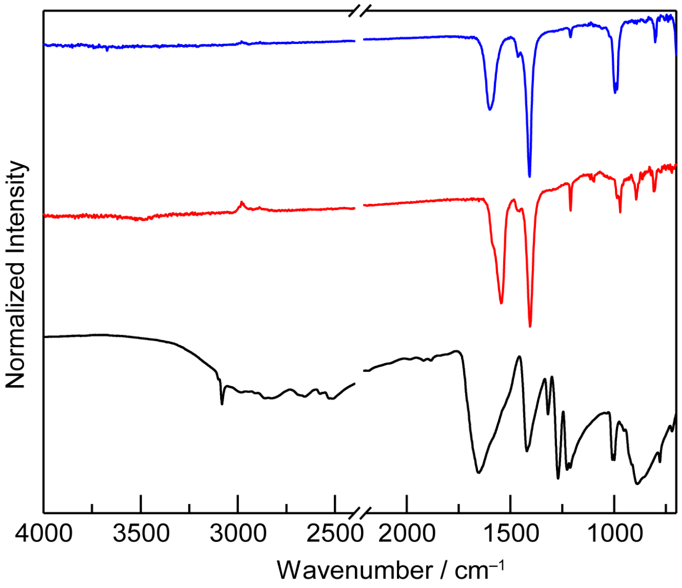

Figure S30. IR spectra (4000–700 cm^{-1} with a break between 2400 and 2200 cm^{-1}) were collected from [Ga(OH)(fum)] (—), [In(OH)(fum)] (—) and H$_2$mfum (—). The mechanochemically obtained samples lack the broad O–H stretching between 2500 and 3300 cm^{-1} and the uncoordinated carbonyl stretching at 1650 cm^{-1}, indicating the formation of an extended framework.

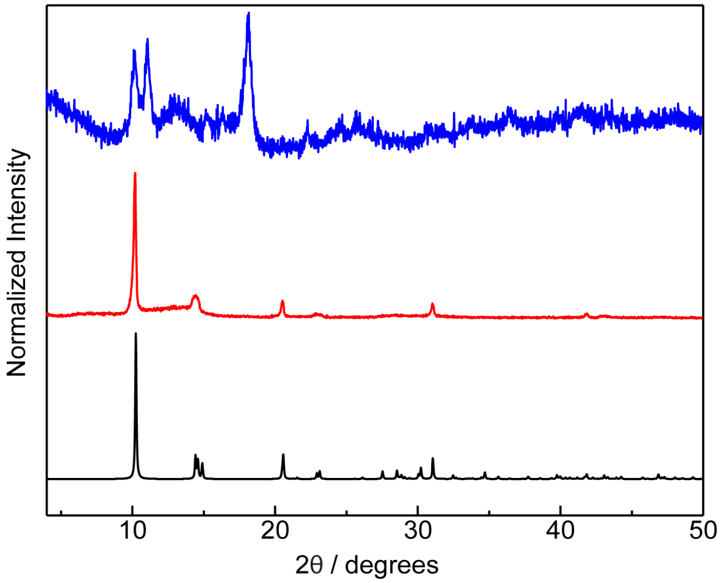

Figure S32. PXRD patterns were collected on the mechanochemically obtained solids by the employment of different gallium(III) precursors, including $Ga_2(SO_4)_3 \cdot 17H_2O$ (—) and $Ga(OAc)_3$ (—), along with stoichiometric amounts of H_2fum and NaOH under the neat condition at 30 Hz for 45 min. Compared against the calculated patterns of [Ga(OH)(fum] (—), the reaction using $Ga_2(SO_4)_3 \cdot 17H_2O$ produces the desired phase of [Ga(OH)(fum].

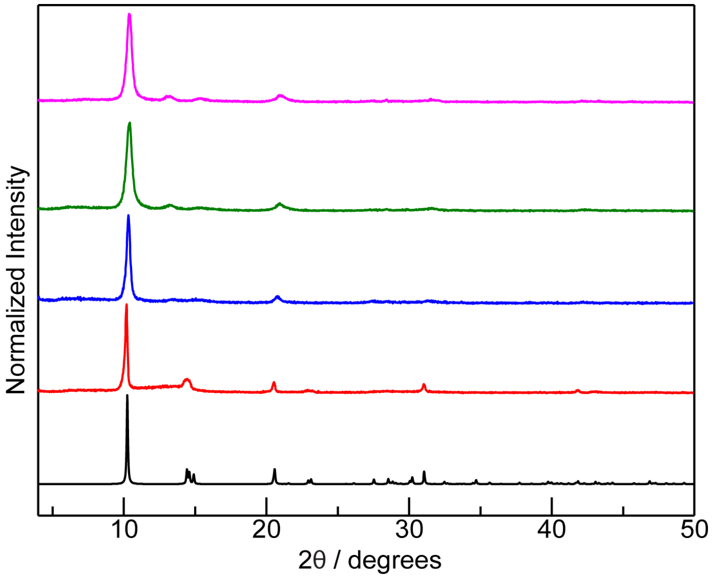

Figure S33. PXRD patterns were collected on the mechanochemically obtained [Ga(OH)(fum)] solids by the employment of various liquid additives including DMF (η = 0.40 μL/mg, —), DMF (η = 0.20 μL/mg, —), and H_2O (η = 0.20 μL/mg, —), as well as the neat condition (—) along with stoichiometric amounts of $Ga_2(SO_4)_3\cdot 17H_2O$, H_2fum and NaOH at 30 Hz for 45 min. Compared against the calculated patterns of [Ga(OH)(fum)] (—), no significant impact can be observed except the narrowest peak width featured by the neat condition.

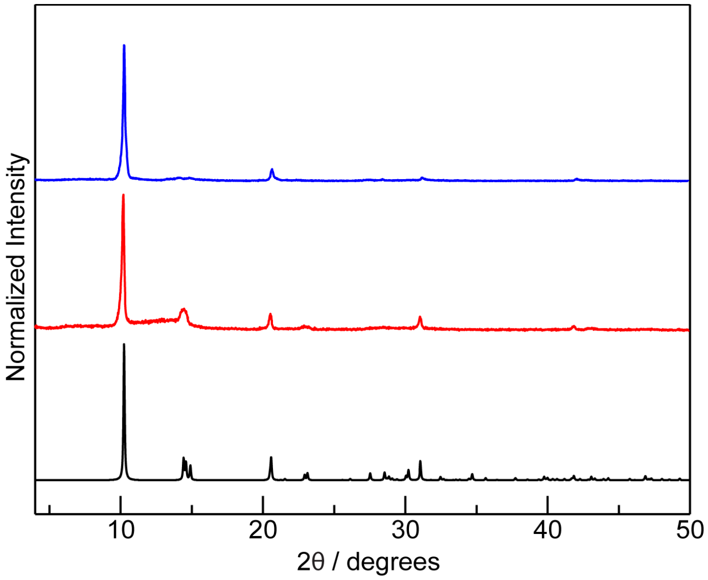

Figure S34. PXRD patterns were collected on the mechanochemically obtained [Ga(OH)(fum)] by the employment of different milling time, including 45 min (—) and 90 min (—), along with stoichiometric amounts of $Ga_2(SO_4)_3{\cdot}17H_2O$, H_2fum and NaOH under neat conditions at 30 Hz.

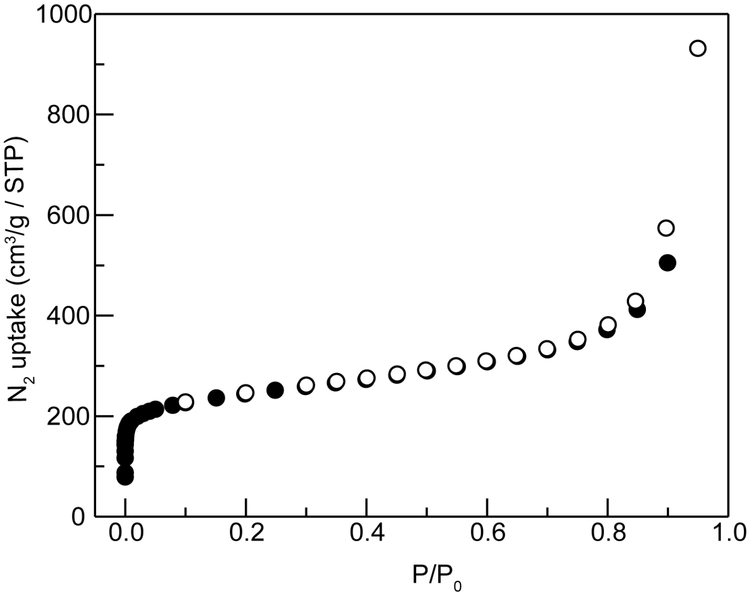

Figure S36. N_2 adsorption isotherm (adsorption (●), desorption (○)) at 77 K was collected from [Ga(OH)(fum)]. The Brunauer-Emmett-Teller (BET) surface area was calculated as 880 m^2/g (P/P_0 = 0.007 to 0.03).

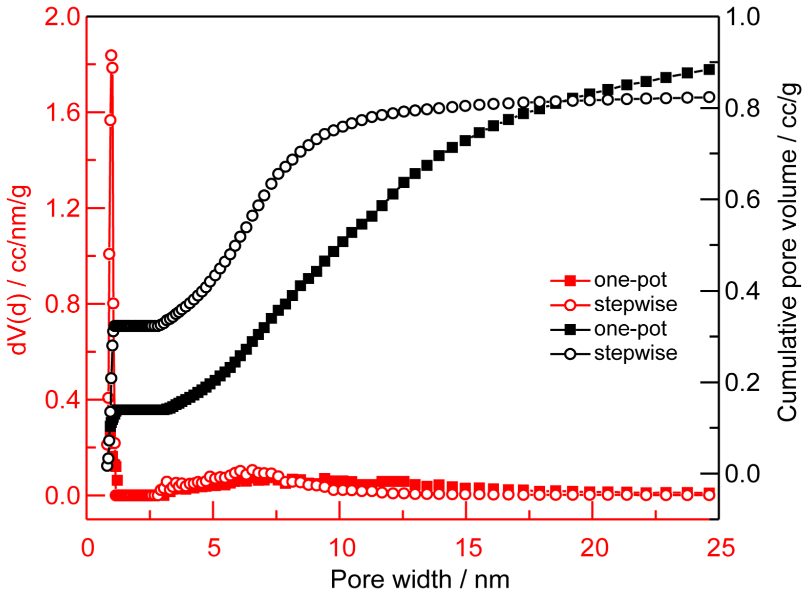

Figure S37. The pore size distribution plots of mechanochemically prepared [Al(OH)(bdc)] are reported by both dV(d) and cumulative pore volume calculated by N_2 adsorption isotherms using the non-local density functional theory (NLDFT).

D. References

1. C. F. Macrae, P. R. Edgington, P. McCabe, E. Pidcock, G. P. Shields, R. Taylor, M. Towler and J. van de Streek, *Journal of Applied Crystallography*, 2006, **39**, 453-457.